

# Crack driving force prediction based on finite element analysis using standard models

Josip Brnic\*, Goran Vukelic<sup>a</sup> and Goran Turkalj<sup>b</sup>

Department of Engineering Mechanics, Faculty of Engineering, University of Rijeka,  
Vukovarska 58, 51000 Rijeka, Croatia

(Received March 6, 2012, Revised October 11, 2012, Accepted October 24, 2012)

**Abstract.** Effect of different crack sizes on fracture criterion of some engineering materials was investigated in this work. Using finite element (FE) method coupled with a newly developed algorithm,  $J$ -integral values for different crack sizes were obtained for single-edge notched bend (SENB) and compact type (CT) specimen. Specimens with initial  $a/W$  ratio from 0.25 to 0.75 varying in crack size in steps of 0.125 were investigated. Several different materials, like 20MnMoNi55, 42CrMo4 and 50CrMo4, usually used in engineering structure, were investigated. For one of mentioned materials, numerical results were compared with experimental and their compatibility is visible.

**Keywords:** crack driving force;  $J$ -integral; finite element method; engineering material

---

## 1. Introduction

Pre-existing defects, imperfections in manufacturing or unfavorable service conditions can cause crack appearance in structures or their components. With cracks growing from micro voids in material to easily detected macro flaws, structural integrity may be threatened. If material exhibits elastic-plastic behaviour, ductile tearing occurs with voids nucleating inside the inclusions or at the boundary inclusion surfaces during material loading under a critical normal stress (Rakin *et al.* 2008). Using fracture toughness test the resistance of material to crack extension ( $\Delta a$ ) can be obtained. The mentioned test may yield a resistance curve ( $R$  curve) where a specific fracture mechanics parameter ( $K$  - fracture toughness,  $J$  -  $J$ -integral, CTOD - crack tip opening displacement) is plotted versus crack extension.  $J$ -integral is usually used when material ahead of crack tip exhibits significant plastic behavior, but it is acceptable also for elastic behavior of material.

Determination of  $J$ - $R$  curves using standardized specimens, such as compact tension (CT) or single-edge notched bend (SENB) specimen, helps in assessing material's structural integrity from fracture mechanics point of view. ASTM E1820 (ASTM 2005) is one of the standardized experimental procedures that regulates  $J$  determination using single specimen test method. Single specimen test method follows elastic unloading compliance technique that uses measured crack

---

\*Corresponding author, Professor, E-mail: [brnic@riteh.hr](mailto:brnic@riteh.hr)

<sup>a</sup>Ph.D., E-mail: [gvukelic@riteh.hr](mailto:gvukelic@riteh.hr)

<sup>b</sup>Professor, E-mail: [turkalj@riteh.hr](mailto:turkalj@riteh.hr)

mouth opening displacement to estimate crack size.

Although  $J$ -integral values are usually obtained in laboratory environment, these procedures can be successfully performed using finite element (FE) method as an addition or even a substitute for costly experiments. This can be taken as a mean motivation for mentioned procedure. Some of the previous work on similar matter includes establishment of local ductile fracture criterion used in modeling of crack growth and  $J$ - $R$  curves simulation, (Margolin and Kostlyev 1998). Wide applicability of  $J$ -integral is shown when  $J$ -integral method, coupled with FE analysis, was successfully used in computing stress intensity factor, (Tiorean and Baltes 2009). Further, using cohesive elements numerical simulation of experimental techniques for  $J$  determination was conducted, (Kozak and Dlouhy 2007). FE models of single-edge notched tension specimens were developed for crack size evaluation using unloading compliance, (Shen and Tyson 2009). In order to understand the process of crack initiation and propagation in ductile materials using CT specimen, FE analysis was conducted on macro, meso and microscale (Saxena and Ramakrishnan 2007). In order to evaluate  $J$ -estimation equation proposed by Kirk and Dodds (1993) for shallow-cracked SENB specimen, two-dimensional FE stress analysis of the same specimen was carried out by Kim and Schwalbe (2001) to result in a modified equation applicable to all crack lengths.

In this paper an attempt has been made in developing an algorithm that calculates  $J$ -integral values. As input algorithm uses stress analysis results from FE simulation of single specimen test method. Resulting values of  $J$ -integral are presented as a measure of crack driving force plotted versus crack extension. This gives an optional mean of  $J$ -integral determination, useful as an addition to FE programs without that capability. Further, numerically predicted  $J$ - $a$  data sets are obtained for several engineering materials.

## 2. Preliminary consideration

$J$ -integral was first introduced by Rice (1968) as a path-independent integral which can be drawn around the tip of a crack and viewed both as an energy release rate parameter and a stress intensity parameter. Two-dimensional  $J$ -integral in its simplest form and with reference to Fig. 1 is given by

$$J = \int_{\Gamma} \left( w dy - T_i \frac{\partial u_i}{\partial x} ds \right) \quad (1)$$

where  $w$  is strain energy density,  $T_i = \sigma_{ij}n_j$  are components of the traction vector,  $u_i$  are the displacement vector components and  $ds$  is a length increment along the contour  $\Gamma$ .

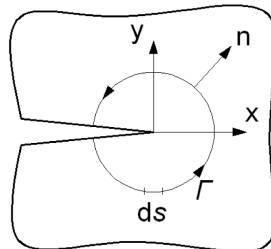


Fig. 1  $J$ -integral arbitrary contour path surrounding the crack tip

When applied to FE models,  $J$ -integral can be written as (Mohammadi 2008)

$$J = \int_{\Gamma} \left\{ \frac{1}{2} \left[ \sigma_{xx} \frac{\partial u_x}{\partial x} + \sigma_{xy} \left( \frac{\partial u_x}{\partial y} + \frac{\partial u_y}{\partial x} \right) \frac{\partial u_x}{\partial x} + \sigma_{yy} \frac{\partial u_y}{\partial y} \right] \frac{\partial y}{\partial \eta} - \left[ (\sigma_{xx} n_1 + \sigma_{xy} n_2) \frac{\partial u_x}{\partial x} + (\sigma_{xy} n_1 + \sigma_{yy} n_2) \frac{\partial u_y}{\partial x} \right] \sqrt{\left( \frac{\partial x}{\partial \eta} \right)^2 + \left( \frac{\partial y}{\partial \eta} \right)^2} \right\} d\eta \quad (2)$$

Using Gauss integration rule along the contour  $\Gamma$  yields

$$J = \sum_{g=1}^{ng} W_g I_g(\xi_g, \eta_g) \quad (3)$$

where  $W_g$  is the Gauss weighting factor,  $ng$  is the number of integration points and  $I_g$  is the integrand evaluated at each Gauss point  $g$

$$I_g = \left\{ \frac{1}{2} \left[ \sigma_{xx} \frac{\partial u_x}{\partial x} + \sigma_{xy} \left( \frac{\partial u_x}{\partial y} + \frac{\partial u_y}{\partial x} \right) \frac{\partial u_x}{\partial x} + \sigma_{yy} \frac{\partial u_y}{\partial y} \right] \frac{\partial y}{\partial \eta} - \left[ (\sigma_{xx} n_1 + \sigma_{xy} n_2) \frac{\partial u_x}{\partial x} + (\sigma_{xy} n_1 + \sigma_{yy} n_2) \frac{\partial u_y}{\partial x} \right] \sqrt{\left( \frac{\partial x}{\partial \eta} \right)^2 + \left( \frac{\partial y}{\partial \eta} \right)^2} \right\}_g \quad (4)$$

Based on these terms, a numerical algorithm was developed in Matlab that uses FE analysis results from integration points of finite elements surrounding crack tip. Evaluating  $J$ -integral values in these points and summing them along a path that encloses crack tip total value of  $J$  is calculated. Since  $J$ -integral values may differ in the vicinity and away from the crack tip, three different paths around crack tip have been defined in each example and their average value was taken as final. A brief mentioning by other researchers of Eqs. (1) to (4) in a  $J$  calculation algorithm is available for centre cracks in adhesive bonded joints (Premchand and Sajikumar 2009).

### 3. Evaluated engineering materials

Materials usually used in engineering practice were investigated in this work: steels 20MnMoNi55, 42CrMo4 and 50CrMo4. Compositions of the mentioned materials are given in Table 1 (Narasaiah *et al.* 2010, Ellerman and Scholtes 2011, Brnic *et al.* 2010), their mechanical properties ( $\sigma_{YS}$  - yield strength,  $\sigma_{TS}$  - tensile strength) in Table 2 and stress-strain curves, valuable for determining elastic-plastic behavior of materials, are given in Fig. 2.

Table 1 Chemical composition of considered materials ( $w_t$  %)

Material	C	Mn	Si	S	Mo	Cr	Ni	P	Rest
20MnMoNi55	0.2	1.25	0.3	0.05	0.5	0.17	0.6	0.01	96.92
42CrMo4	0.43	0.65	0.26	0.02	0.16	1.07	0.19	0.02	97.2
50CrMo4	0.49	0.74	0.26	0.03	0.19	0.99	-	0.02	97.28

Table 2 Mechanical properties of considered materials

Material	$\sigma_{YS}$ [MPa]	$\sigma_{TS}$ [MPa]
20MnMoNi55	490	620
42CrMo4	650	1000
50CrMo4	1090.2	1146.9

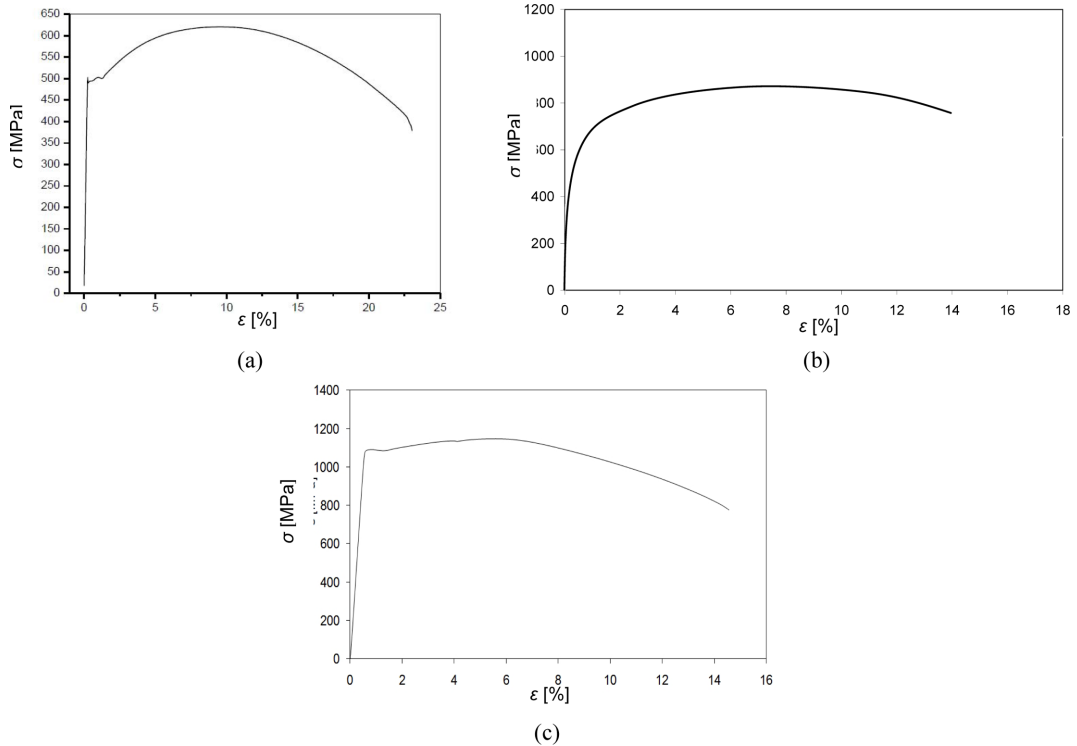


Fig. 2 Stress-strain curve for (a) 20MnMoNi55 (Narasaiah *et al.* 2010), (b) 42CrMo4 (Ellerman and Scholtes 2011), (c) 50CrMo4 (Brnic *et al.* 2010)

#### 4. Finite element analysis and $J$ -integral calculation

Experimental single specimen test method following elastic unloading compliance technique was numerically simulated in order to determine  $J$  values. This test method (ASTM 2005) uses measured crack mouth opening displacement to estimate growing crack size. Collected  $J$  values can be plotted versus crack extension, obtaining in that way  $J$  resistance curves.

Using Ansys FE models of two types of specimen, CT and SENB, usually used in single specimen test method were defined. Geometry was defined according to Fig. 3 (ASTM 2005).

Specimens with initial  $a/W$  ( $W = 50$  mm) ratio from 0.25 to 0.75 varying in steps of 0.125 were investigated. Two-dimensional FE models of specimens were developed in Ansys, Fig. 4. Material behavior was considered to be multilinear isotropic hardening type. FE models of specimens were meshed with 8-node isoparametric quadrilateral elements. In non-linear fracture problems, the

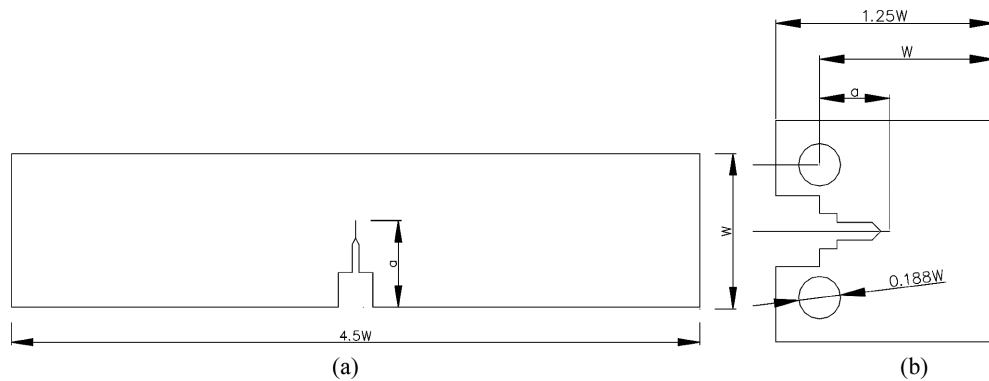


Fig. 3 Specimens according to ASTM E1820 (a) Single-edge notched bend (SENB) specimen, (b) Compact tension (CT) specimen

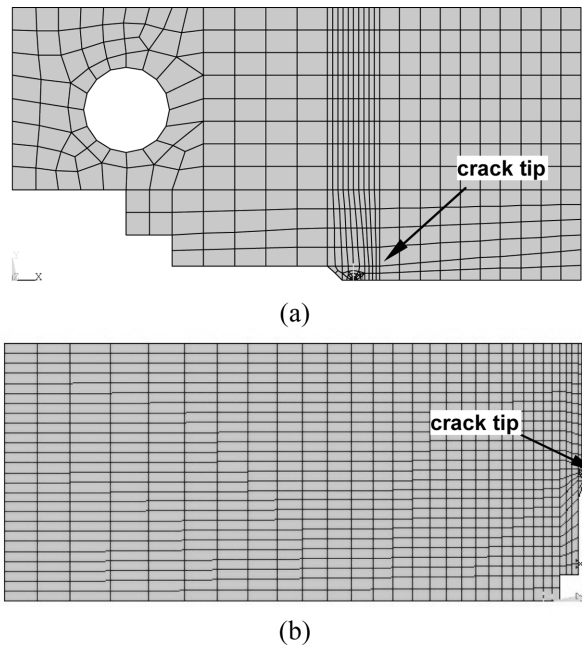


Fig. 4 FE mesh of (a) CT specimen, (b) SENB specimen

mesh must be refined in the regions where yielding occurs in order to capture the existing high deformation gradients (de Araujo *et al.* 2008). Quasi-static load was imposed on specimens to simulate compliance procedure of single specimen test method. Crack propagation was simulated using node releasing technique. With this in mind, it is necessary to ensure that size of the finite elements (i.e., distance between the nodes that are to be released) corresponds to desired measure of crack extension,  $\Delta a$ .

Only half of the specimen structure was modeled because of its symmetry through the crack. Stress analysis was run for every example (CT, SENB), and resulting set of stresses and strains on

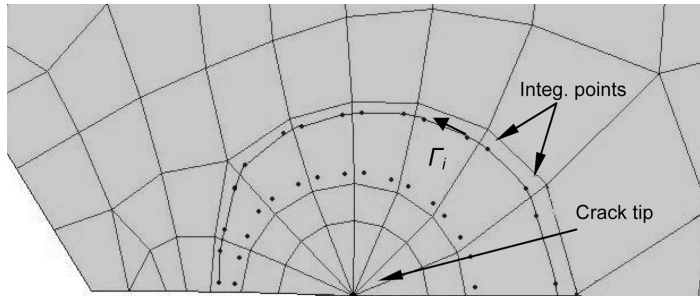


Fig. 5 Single  $J$ -integral path  $\Gamma_i$  surrounding crack tip through finite element integration points

integration points was recorded along with a nodal displacements. In particular it is important to record stresses and strains in the integration points of elements through which the path of the  $J$ -integral passes. Stress analysis results in the integration points of selected elements are used to calculate the contribution of each element to the path. Path passes through two of the four integration points of each finite element. Summing the values of  $dJ$ , contribution of each element to  $J$ , total value of  $J$ -integral is calculated. As mentioned before,  $J$ -integral values may differ in the vicinity and away from the crack tip. Because of that three different paths around crack tip have been defined in each example and their average value was taken as final, Fig. 5.

## 5. Results and discussion

In order to verify algorithm for  $J$ -integral calculation,  $J$  values were first determined for different crack sizes of SENB specimen made of 20MnMoNi55 steel and compared with available experimental results (Narasaiah *et al.* 2010). This comparison is presented in Fig. 6 using  $J$  as a measure of crack driving force and plotting it against crack extension. Good correspondence of numerically predicted and available experimental results gives confidence in using developed algorithm for evaluating  $J$  values of other materials.

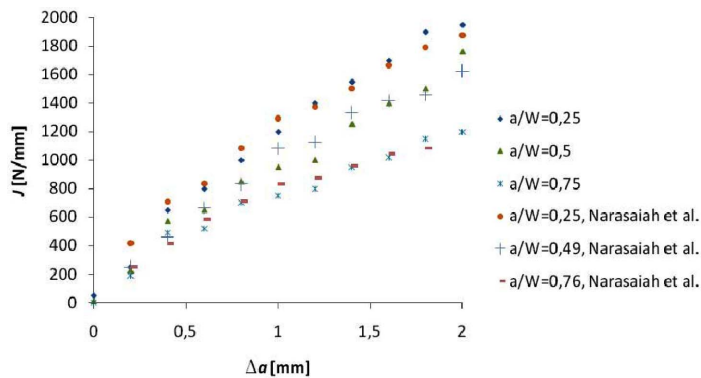


Fig. 6 Comparison of numerically predicted and experimentally obtained  $J$ -integral values vs. crack extension ( $\Delta a$ ) for SENB specimen made of 20MnMoNi55 steel

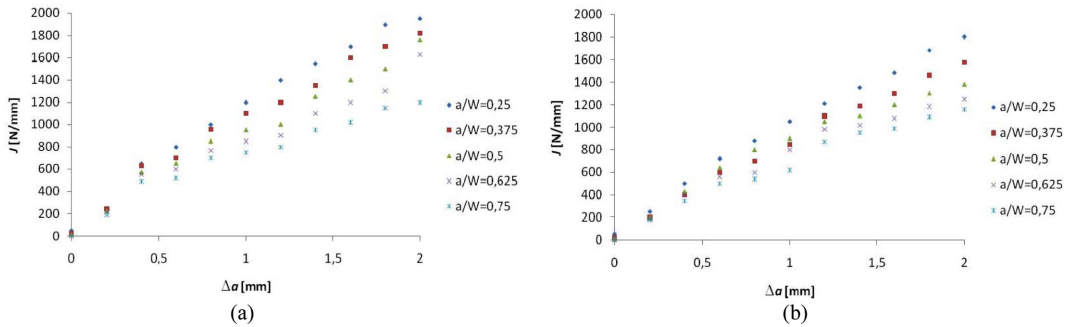


Fig. 7 20MnMoNi55 steel, predicted  $J$  values for  $\Delta a$  (a) SENB specimen, (b) CT specimen

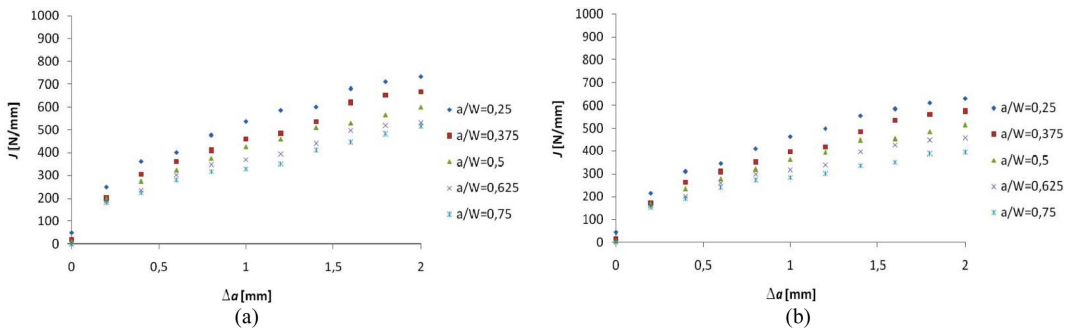


Fig. 8 42CrMo4 steel, predicted  $J$  values for  $\Delta a$  (a) SENB specimen, (b) CT specimen

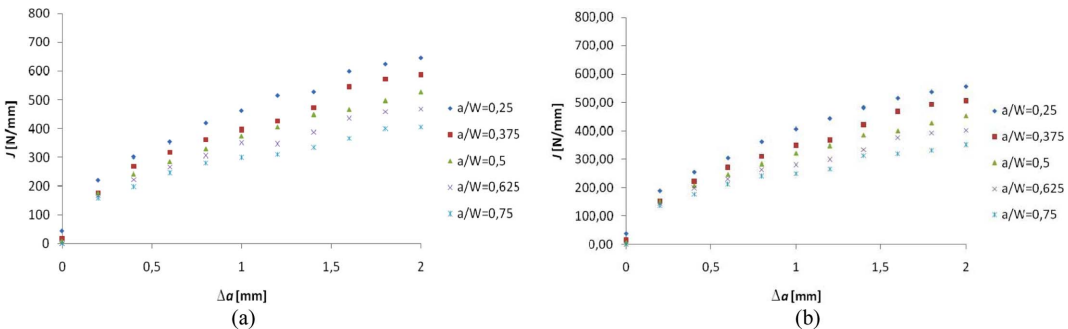


Fig. 9 50CrMo4 steel, predicted  $J$  values for  $\Delta a$  (a) SENB specimen, (b) CT specimen

Finally, numerically obtained  $J$  values are presented as a measure of crack driving force versus crack growth size ( $\Delta a$ ) for a range of considered materials, specimens and crack sizes, Figs. 7, 8 and 9. Observing resulting values of  $J$ -integral it can be noted that 20MnMoNi55 steel has higher  $J$  values than 42CrMo4 or 50CrMo4 steel. Besides, using CT specimen gives more conservative results than SENB specimen. Also, it is noted that higher  $a/W$  ratios correspond with lower critical toughness values of materials and vice versa which matches previous results of other authors (Narasaiah *et al.* 2010).

## 6. Conclusions

Numerical algorithm, based on FE stress analysis, was developed for  $J$ -integral calculation. Results obtained using the mentioned routine show good compatibility with available experimental results for 20MnMoNi55 steel (Narasaiah *et al.* 2010), Fig. 6. This gives confidence in using developed algorithm for evaluating  $J$  values of other materials, 42CrMo4 and 50CrMo4, for which experimental results were not available to authors.

So obtained  $J$  values provide an insight in values of crack driving force for specimens made of different materials and containing a range of crack sizes. Extensive experimental procedures can be reduced when having numerical results as a starting point in the investigation of  $J$  values for new materials. Such results can be of great help in the process of material selection during the design of structures.

Further research can concentrate on applying algorithm on more different materials and types of specimens proposed in (ASTM 2005), as well as applying on numerical models of real cracked structures and components.

## Acknowledgements

The research presented in this paper was realized within the scientific project financially supported by the Ministry of Science, Education and Sport of the Republic of Croatia. Also, the authors would like to express their gratitude to staff of Material Testing Laboratory of Department of Materials at the Faculty of Engineering Rijeka for their investigation in testing of material chemical composition.

## References

- American Society for Testing and Materials (ASTM) (2005), Standard Test Method for Measurement of Fracture Toughness, E1820, ASTM, Baltimore.
- Brnic, J., Canadija, M., Turkalj, G. and Lanc, D. (2010), "50CrMo4 steel-determination of mechanical properties at lowered and elevated temperatures, creep behavior and fracture toughness calculation", *J. Eng. Mater. Technol.*, **132**, 021004-1-021004-6.
- Dense de Araujo, T., Roehl, D. and Martha, L.F. (2008), "An adaptive strategy for elastic-plastic analysis of structures with cracks", *J. Braz. Soc. Mech. Sci. Eng.*, **30**(4), 341-350.
- Ellerman, A. and Scholtes, B. (2011), "The bauschinger effect in different heat treatment conditions of 42CrMo4", *Int. J. Struct. Chang. Solid.*, **3**(1), 1-13.
- Kim, Y.J. and Schwalbe, K.H. (2001), "On experimental J estimation equations based on CMOD for SE(B) specimens", *J. Test. Eval.*, **29**, 67-71.
- Kirk, M.T. and Dodds, R.H., Jr. (1993), "J and CTOD estimation equations for shallow cracks in single edge notch bend specimens", *J. Test. Eval.*, **21**, 228-238.
- Kozak, V. and Dlouhy, I. (2007), "J-R curve prediction using cohesive model and its sensitivity to a material curve", Transactions of SMiRT 19, Toronto, G06/4.
- Margolin, B.Z. and Kostylev, V.I. (1998), "Analysis of biaxial loading effect on fracture toughness of reactor pressure vessel steels", *Int. J. Pres. Ves. Pip.*, **75**(8), 589-601.
- Mohammadi, S. (2008), *Extended Finite Element Method*, Blackwell Publishing, Singapore.
- Narasaiah, N., Tarafder, S. and Sivaprasad, S. (2010), "Effect of crack depth on fracture toughness of

- 20MnMoNi55 pressure vessel steel”, *Mater. Sci. Eng. A*, **527**, 2408-2411.
- Premchand, V.P. and Sajikumar, K.S. (2009), “Fracture analysis in adhesive bonded joints with centre crack”, *Proceedings of the 10th National Conference on Technological Trends*, Trivandrum, **1**, 45-50.
- Rakin, M., Gubelj, N., Dobrojevic, M. and Sedmak, A. (2008), “Modelling of ductile fracture initiation in strength mismatched welded joint”, *Eng. Fract. Mech.*, **75**(11), 3499-3510.
- Rice, J.R. (1968), “A path independent integral and the approximate analysis of strain concentration by notches and cracks”, *J. Appl. Mech.*, **35**, 379-386.
- Saxena, S. and Ramakrishnan, N. (2007), “A comparison of Micro, Meso and Macroscale FEM analysis of ductile fracture in a CT specimen”, *Comp. Mater. Sci.*, **39**(1), 1-7.
- Shen, G. and Tyson, W.R. (2009), “Crack size evaluation using unloading compliance in single-specimen single-edge-notched tension fracture toughness testing”, *J. Test. Eval.*, **37**(4), 347-357.
- Tierean, M. and Baltes, L. (2009), “Computing of stress intensity factor using j-integral method with F.E.A.”, *Annals of DAAAM 2009 & Proceedings of the 20th Int. DAAAM Symposium*, Vienna, 1105-1106.